Design Improvement of a Commercial Impingement Two-Phase Cold Plate Used for High Heat Flux Applications

Najmeh Fallahtafti, Cong Hiep Hoang, Yaser Hadad, Srikanth Rangarajan, Scott Schiffres, Bahgat Sammakia
Department of Mechanical Engineering, Binghamton University-SUNY, Binghamton, NY, USA

Email: nfallah1@binghamton.edu

Abstract

Heat fluxes in the data center have been increasing significantly due to the rise in advanced technologies such as Artificial Intelligence (AI), 5G, high-performance computing (HPC), and machine learning. The traditional air-cooling technology cannot handle high heat fluxes and requires a bigger heat sink; therefore, hindering high heat flux and high density in the data center. Two-phase cooling schemes are particularly appropriate for high heat flux situations because of their enhanced heat transfer coefficients and the non-linear relationship between heat flux and surface-to-fluid temperature difference. In this study, an experimental setup was developed to characterize and optimize the thermo-hydraulic performance of two-phase cooling cold plates intended for high heat flux applications. An improvement of 12% in thermal performance was obtained by cutting the original fins and creating mini-channels perpendicular to the original microchannels without a significant pressure drop penalty.

1. Introduction

Ever-shrinking size of electronic systems necessitates higher circuit integration per unit area, which results in a rapid increase in heat generation density. Global data centers consumed around 200 billion kWh/year [1], which corresponded to 1.3% of total global electricity usage. About 33% of this power is used for cooling in data centers [2]. The heat flux in electronic devices continues to increase and already exceeded the cooling capacity of air-cooling technology. Therefore, practical and efficient heat removal solutions that can make the system works at a safe operating temperature and ensure its reliability is required [3]. Liquids with high specific heat capacity, density, and incompressibility, can absorb, store, and carry a larger amount of thermal energy than air, making liquid cooling an attractive solution [4]. By adopting direct liquid cooling, not only is the heat flux and high-power demands met, but the reliability of the electronic devices is greatly improved [5]. There are two methods of liquid cooling: single-phase and two-phase liquid cooling. Single-phase cooling with water is the most popular liquid cooling method in data centers [6], [7]. It is reported that the highest heat transfer rate of single-phase cooling with water can be up to 1150 W for a 27 $cm2$ chip [8], [9]. However, high temperature gradient on the chip surface and potential consequences of water leak are disadvantages of single-phase cooling with water. On the other hand, two-phase cooling systems, using dielectric refrigerants, can address power densities more than two times of single-phase systems [8] and eliminates the short circuit risk caused by a fluid leak. Two-phase cooling benefits the latent heat, not only resulting in larger cooling capacities compared to single-phase cooling, but it also provides more uniform surface temperature due to the boiling of coolant slightly above the saturation temperature.

Jet-impingement and parallel flow are two of the most common flow configurations for two-phase cooling in electronic applications. Impingement microchannel cold plates in two-phase cooling can dissipate very high heat fluxes and results in lower pressure drop compared to parallel flow microchannel cold plate. Hadad et al. [10], [11] studied the hydraulic and thermal performance of impingement microchannel water-cooled cold plates numerically. Their results show that by replacing parallel microchannel cold plates with impingement microchannel cold plates, a considerable reduction in pressure drop is observed without any significant thermal performance penalty. Myung et al. [12] studied single-phase and two-phase cooling performance of a hybrid microchannel/slot-jet impingement module using HFE-7100 as the coolant. The combination of microchannel and slot-jet can enhance surface temperature uniformity with less than 2℃ degree of the temperature gradient. Wan et al. [13] experimentally investigated the performance of four types of pin fin arrays in two-phase cooling: square, circular, diamond, and streamlined. Test results showed that the square micro pin fins presented the best boiling heat transfer, followed by circular and streamlined ones.

Although dielectric coolants have lower thermal conductivity and higher prices than water, they are electrically non-conductive and therefore preferred when working with sensitive electronics. On the condition of coolant leakage, dielectric fluids can prevent circuits from being shorted and electrical discharge. Novec/HFE 7000 is a coolant with a low global warming potential and a low boiling point of 34℃ at 1 atm. Its low boiling point and pressure allow IT devices to operate at low junction temperature and acceptable pumping power. Moreover, this low boiling point is a reason why this coolant attracts attention for two-phase electronics cooling applications. Yang et al. [14] investigated flow boiling heat transfer of HFE 7000 in nanowire-coated microchannels. They concluded that at heat fluxes lower than 120 $W/cm2$, the heat transfer coefficient and critical heat flux (CHF) were enhanced by 344% and 14.9%, respectively. The enhancement of the heat transfer coefficient was due to the thin-film evaporation in the entire channels when the flow pattern was dominated by the capillarity-induced annular flow.

The objective of this study is to improve the thermal performance of a two-phase microchannel impingement commercial cold plate by changing its original architecture. Indeed, convective flow boiling and number of bubble sites increase by creating mini-channels perpendicular to the original microchannels of the cold plate.

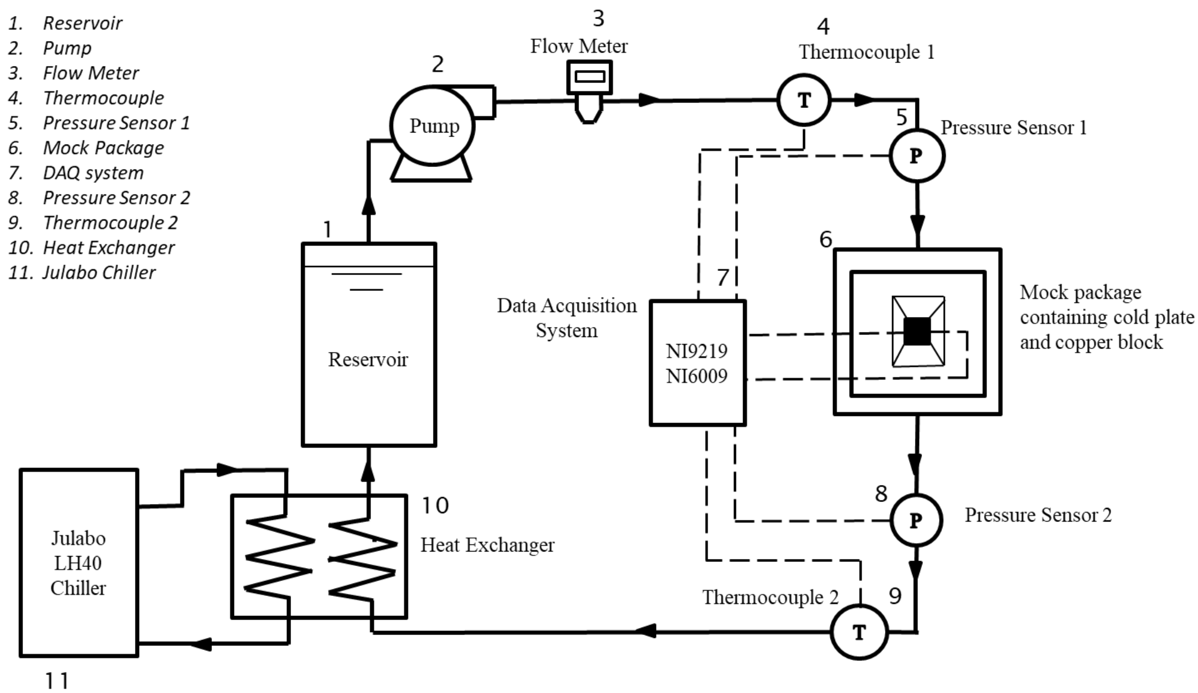

Figure 1: Schematic of the setup

2. Experimental setup and heat sink design

2.1. Flow Loop and Test Section

Fig.1 shows a schematic of the experimental setup. A gear pump circulates the coolant through the components of the setup. A volumetric flow meter placed right before the inlet of the cold plate measures the flow rate. Two T-type thermocouples at the inlet and outlet of the cold plate quantify the inlet and outlet coolant temperatures. Two pressure sensors at the inlet and outlet of the cold plate are used to measure the pressure drop across it. Mock package contains a cold plate and a copper block (with thermal conductivity of 380 $W/m.\ K$) which simulates a chip. As Fig. 2 illustrates, the cold plate is located on top of the copper block and is held with the help of a weight seat for applying a pressure of 15 psi to ensure an adequate surface contact between the cold plate and top surface of the copper block. To minimize contact thermal resistance, a thermal interface material (Kryonaut Thermal-Grizzly) with

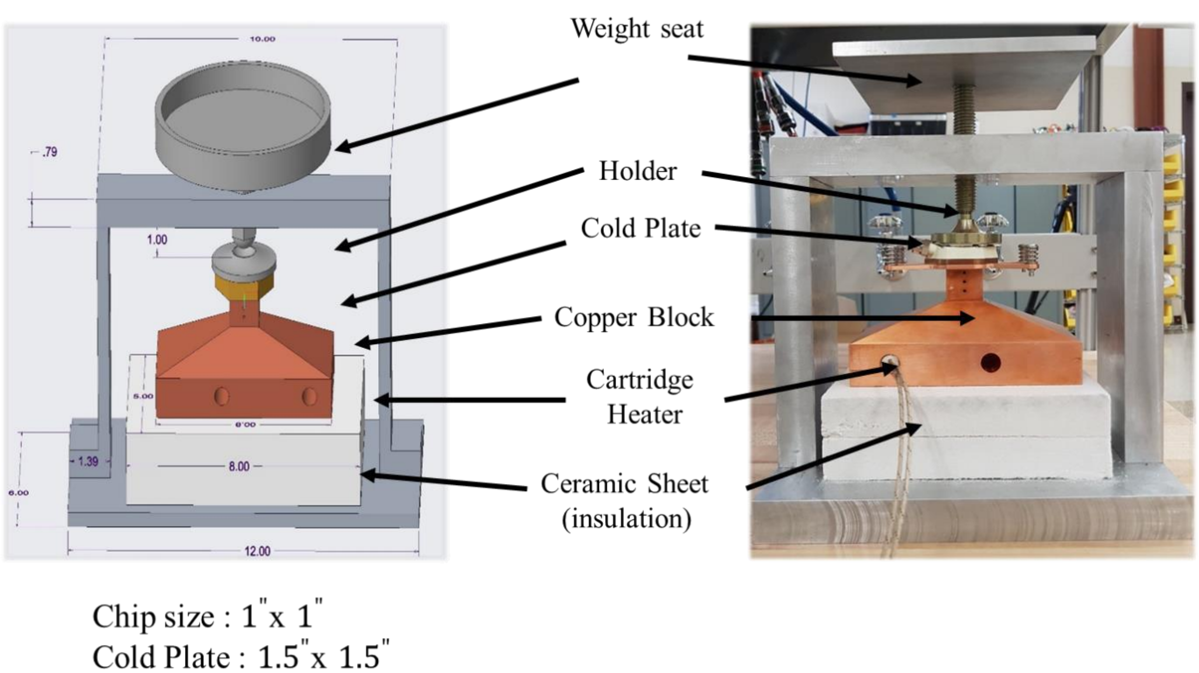

Figure 2: Mock package design

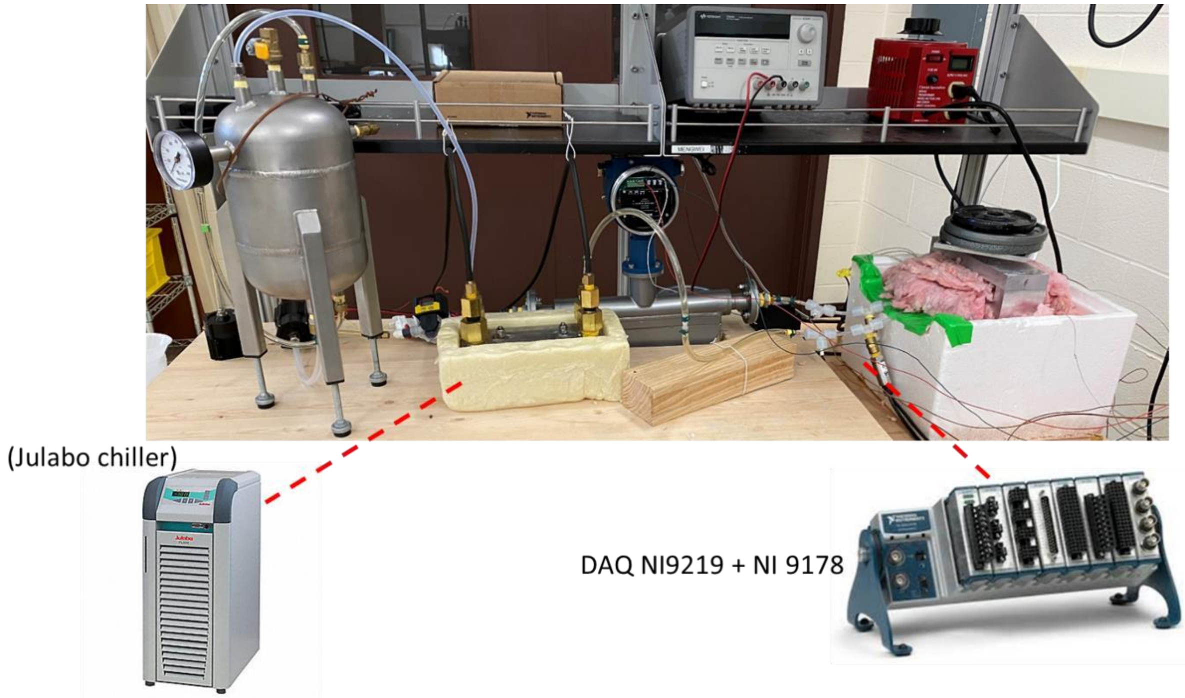

Figure 3: A photo of the setup

Instruments	Measurand	Uncertainty	DAQ module
Pressure Gauges (Omega): PX309050A5V	Pin, Pout	$\pm 0.8 kPa$	NI-USB-6009
Coriolis Flow Meter (TacticalFlowMeter): TFM-1001	Flow Rate	± 0.2%	NI 9219
T-type thermocouples: laboratory made	Tin, Tout, Tb	±0.2 ºC	NI 9219
Thermocouple (Omega): TJ36CASS-116E-2-CC	Heat Flux Measurement	±0.2 ºC	NI 9219

Table 1. Measurement instruments and uncertainty.

thermal conductivity of 12.5 $W/m.K$ is used to attach the cold plate to the top of the copper block. The copper block is insulated from the bottom and sides with the help of a ceramic sheet insulator and a fiberglass insulation layer, respectively. The desired power is supplied by four cartridge heaters embedded at the bottom sides of the copper block and connected to an AC power supply. Each cartridge heater can deliver 400 W of heat. The actual heat supplied to the cold plate is calculated by applying the Fourier law of conduction to the temperatures measured by three K-type thermocouples placed in the neck of the copper block. The outlet coolant is subcooled by means of a heat exchanger (connected to a chiller) preceding the reservoir. All sensors are connected to data acquisition to gather data in a LabVIEW program. A photo of the experimental setup is illustrated in Fig.3. The uncertainty of the measurement instruments is listed in Table 1. Novec/HFE 7000 is chosen as the coolant. The thermophysical properties of Novec/HFE 7000 is presented in Table 2. Novec 7000 is a non-ozone depleting fluid

2.2. Heat Sink Design

The original microchannel cold plate's fin geometry and manifold are shown in Fig. 4. The original fin thickness and channel width are both 0.1 mm and the fin height is 3 mm. As shown in Fig. 4 (b), the manifold consists of 34 inlet jets with

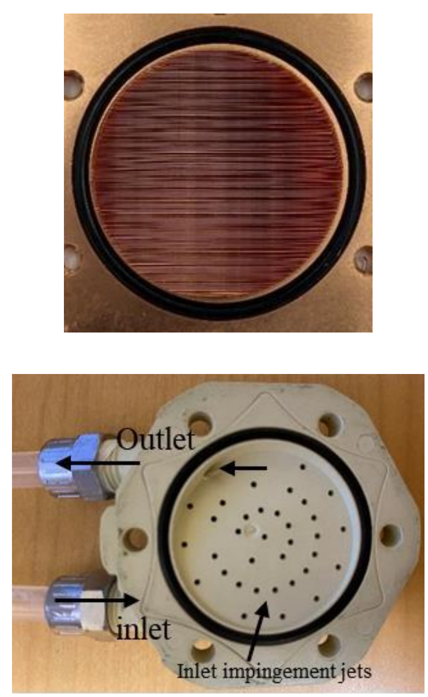

Figure 4: Original microchannels from top view

	ρ (kg/m^3)	k $(W/m.\ K)$	c_p $(J/kg.\ K)$	μ $(kg/m.\ s)$	GWP
Novec/HFE 7000	1400	0.075	1300	0.00045	420

Table 2. Thermophysical properties of Novec/HFE 7000

the diameter of 1 mm. Coolant impinges through these jets on the top of the fins and leaves the cold plate from the outlet on the top. The distance between the fin tip and jets is 0.3 mm as mentioned in our previous work [15]. The improved design is obtained by machining 19 mini-channels of 0.5 mm width (wch) and 1 mm distance (d) perpendicular to the original microchannels. Fig.5 (b) illustrates the dimensions of the improved design.

3. Results and discussions

3.1. Effect of coolant inlet temperature

To investigate the effect of coolant inlet temperature, an experiment was conducted with coolant inlet temperature varying from 25°C to 48°C and heat flux was increased from 7 $W/cm2$ to 71 $W/cm2$. Flow rate was maintained at a constant value of 1 LPM. The effect of inlet temperature was studied on the two designs mentioned in section 2.2. Thermal and hydraulic performances of the two designs were evaluated by thermal resistance and pressure drop according to Eqs.1 and 2, respectively. A time period of about 40 minutes was spent before gathering each data point to make sure that the setup operated in a stable condition. It is observed in Fig. 6 and Fig. 7 that thermal resistance remains almost constant at low heat fluxes when the flow is single-phase. After the onset nucleate boiling point (ONB), thermal resistance decreases with heat flux due to nucleate boiling with higher vapor quality. Thermal resistance decreases by increasing inlet temperature for a constant flow rate in a two-phase flow regime for both cold plate designs. The reduction of thermal resistance with inlet temperature is attributed to the higher vapor quality that is generated when coolant moves through the cold plate at close-to-saturation temperatures. Cold plate's twophase pressure drop increases by increasing heat flux due to more bubble generation. It is also shown that ONB occurs earlier at higher inlet temperatures for the same reason. On the other hand, by increasing coolant inlet temperature and consequently higher vapor quality, pressure drop rises as shown in Figs. 8 and 9.

Figure 5: Improved deisgn, top – top view, bottom – perspective view

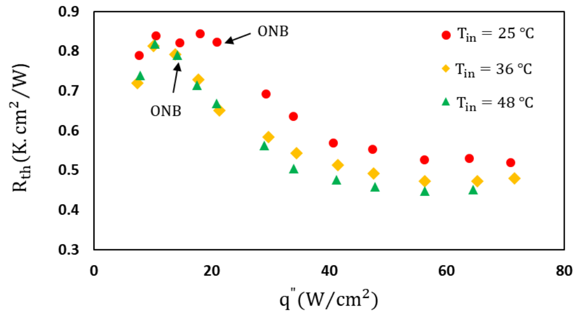

Figure 6: The effect of coolant inlet temperature on thermal resistance

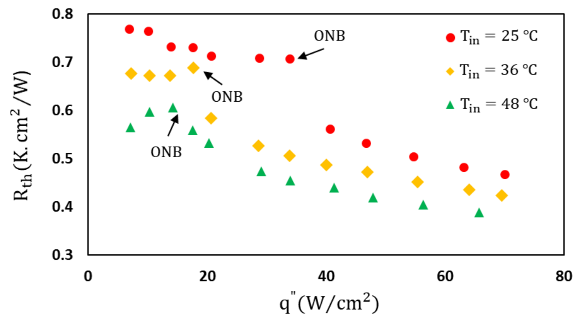

Figure 7: The effect of coolant inlet temperature on thermal resistance of improved design.

$$R_{th} = \frac{T_b - T_{in}}{q''} \quad [1]$$

Tb is average temperature of the cold plate's base and Tin is coolant inlet temperature. q" is heat flux generated by the chip.

$$\Delta P = P_{in} - P_{out} \quad [2]$$

Pin and $Pout$ are pressure at the inlet and outlet, respectively.

3.2. Comparison of two cold plates designs' performance

A comparison between the thermal performance of the two cold plate designs is presented in Fig 10 at a coolant inlet temperature of 36 °C and a flow rate of 1 LPM. As it can be seen, thermal resistance decreases by creating channels with a width of 0.5 mm perpendicular to the original microchannels. Average reductions of 11% and 9% in thermal resistance are observed for singlephase and two-phase, respectively by switching from the original design to the improved one. Since the original channels are too narrow (0.1 mm), convective flow boiling cannot be formed there. Indeed, low-velocity flow with a bubble generation similar to pool boiling is formed in channels and the major part of the flow bypasses the channels

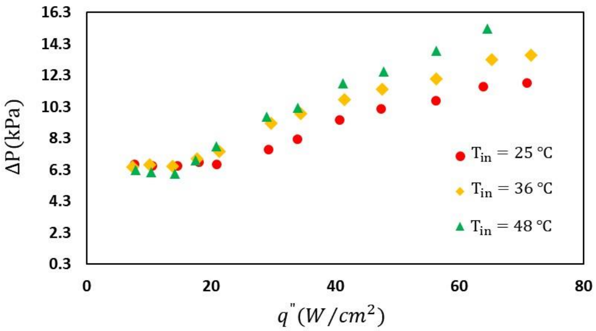

Figure 8: The effect of coolant inlet temperature on pressure drop of original design.

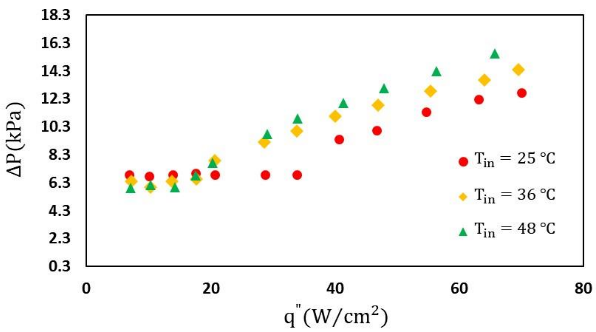

Figure 9: The effect of coolant inlet temperature on thermal pressure drop of improved design.

and leaves the cold plate to the exit. Creating the channels perpendicular to the original narrow channels, causes convective flow boiling in the channel network which results in lower thermal resistance. In the single-phase regime the thermal resistance decreases by creating the mini-channels as they let the channel network exchange heat by forced convection. Low-velocity flow in the narrow deep channels of the original design makes conduction heat transfer dominant which is significantly inefficient than forced convective heat transfer. Fig. 11 demonstrates that the pressure drop does not show significant sensitivity to the fin geometry since the major pressure drop occurs in the manifold's small jets.

4. Conclusion

In this study, a commercial two-phase cold plate was improved in design by machining minichannels perpendicular to its original microchannels. The obtained experimental results showed a significant improvement in thermal performance of the cold plate both in single and two-phase without a considerable hydraulic performance reduction. Indeed, created channels fortified convective heat transfer through the channel network and prevent the coolant to skip it before leaving the cold plate. Although by machining the mini-channels the cold plate lost some heat transfer surface area, the number of bubble sites and channel Reynolds number increased. The performance of both designs was estimated for different coolant inlet temperatures and chip powers. As expected, the thermal resistance did not change remarkably with power in a single phase. However, it sharply decreased by increasing power in two-phase regime. Two-phase thermal resistance decreased by increasing coolant inlet temperature while the pressure drop rose.

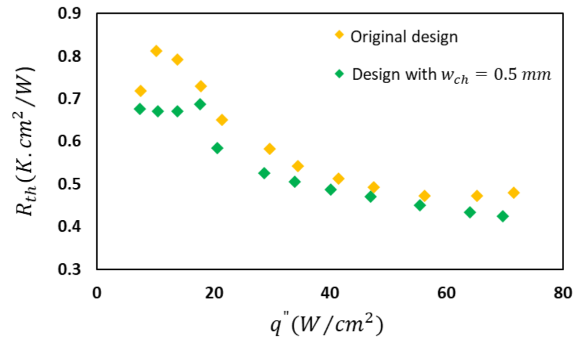

Figure 10: Comparison of thermal resitance of two designs studied.

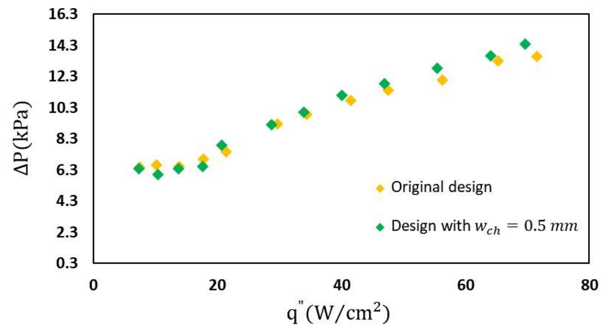

Figure 11: Comparison of pressure drop of two designs studied.

Acknowledgement

This work is supported by SRC (Task 2878.006). S.N.S. acknowledges the NSF Award IIP1738793 and the Integrated Electronics Engineering Center (IEEC) at the State University of New York at Binghamton. The IEEC is a New York State Center for Advanced Technology with funding from New York State through the Empire State Development Corporation. Authors would like to acknowledge A. Heydari from NVIDIA, M. Seymour from Future Facilities, and C. Arvin from IBM for their useful comments and guidance through the course of this study.

References

1. N. Jones, "How to stop data centres from gobbling up the world's electricity," Nature, vol. 561, no. 7722, pp. 163–166, Sep. 2018, doi: 10.1038/d41586-018-06610-y.
2. S. Garimella, T. Persoons, J. Weibel, and L.-T. Yeh, "Technological Drivers in Data Centers and Telecom Systems: Multiscale Thermal, Electrical, and Energy Management," CTRC Res. Publ., Jan. 2013, doi: http://dx.doi.org/10.1016/j.apenergy.2013.02.047.
3. B. Agostini, M. Fabbri, J. E. Park, L. Wojtan, J. R. Thome, and B. Michel, "State of the Art of High Heat Flux Cooling Technologies," Heat Transf. Eng., vol. 28, no. 4, pp. 258–281, Apr. 2007, doi: 10.1080/01457630601117799.
4. S. Alkharabsheh et al., "A Brief Overview of Recent Developments in Thermal Management in Data Centers," J. Electron. Packag. Trans. ASME, vol. 137, Dec. 2015, doi: 10.1115/1.4031326.
5. R. Schmidt, "Packaging of New Servers - energy efficiency aspects-," p. 35, 2006.

6. “Comparing Liquid Coolants From Both A Thermal And Hydraulic Perspective,” Electronics Cooling, Aug. 09, 2006. https://www.electronicscooling.com/2006/08/comparing-liquid-coolants-from-both-a-thermal-and-hydraulicperspective/ (accessed Jan. 13, 2022).
7. T. Gao et al., “A study of direct liquid cooling for high-density chips and accelerators,” in 2017 16th IEEE Intersociety Conference on Thermal and Thermomechanical Phenomena in Electronic Systems (ITherm), May 2017, pp. 565–573. doi: 10.1109/ITHERM.2017.7992537.
8. A. Kheirabadi and D. Groulx, “Cooling of Server Electronics: A Design Review of Existing Technology,” Appl. Therm. Eng., vol. 105, Mar. 2016, doi: 10.1016/j.applthermaleng.2016.03.056.
9. B. Rimbault, C. T. Nguyen, and N. Galanis, “Experimental investigation of CuO–water nanofluid flow and heat transfer inside a microchannel heat sink,” Int. J. Therm. Sci., vol. 84, pp. 275–292, Oct. 2014, doi: 10.1016/j.ijthermalsci.2014.05.025.
10. Y. Hadad et al., “Performance analysis and shape optimization of a water-cooled impingement micro-channel heat sink including manifolds,” Int. J. Therm. Sci., vol. 148, p. 106145, Feb. 2020, doi: 10.1016/j.ijthermalsci.2019.106145.
11. Y. Hadad et al., “Performance Analysis and Shape Optimization of an Impingement Microchannel Cold Plate,” IEEE Trans. Compon. Packag. Manuf. Technol., vol. 10, no. 8, pp. 1304–1319, Aug. 2020, doi: 10.1109/TCPMT.2020.3005824.
12. M. K. Sung and I. Mudawar, “Single-phase and two-phase cooling using hybrid microchannel/slot-jet module,” Int. J. Heat Mass Transf., vol. 51, no. 15–16, pp. 3825–3839, Jul. 2008, doi: 10.1016/j.ijheatmasstransfer.2007.12.015.
13. W. Wan, D. Deng, Q. Huang, T. Zeng, and Y. Huang, “Experimental study and optimization of pin fin shapes in flow boiling of micro pin fin heat sinks,” Appl. Therm. Eng., vol. 114, pp. 436–449, Mar. 2017, doi: 10.1016/j.applthermaleng.2016.11.182.
14. F. Yang, W. Li, X. Dai, and C. Li, “Flow boiling heat transfer of HFE-7000 in nanowirecoated microchannels,” Appl. Therm. Eng., vol. 93, pp. 260–268, Jan. 2016, doi: 10.1016/j.applthermaleng.2015.09.097.
15. C. H. Hoang et al., “Hybrid microchannel/multi-jet two-phase heat sink: A benchmark and geometry optimization study of commercial product,” Int. J. Heat Mass Transf., vol. 169, p. 120920, Apr. 2021, doi: 10.1016/j.ijheatmasstransfer.2021.120920.